International Journal of Engineering Research Excellence and Applied Science (IJEREAS)

Volume-II (Issue 2) - June 2024 ISSN: 3048-5355

SIMULATION AND DESIGN OF GRID CONNECTED SOLAR CHARGER FOR ELECTRIC VEHICLE

Sonu Rani[1], Pankaj Kumar[2]
[1]M. Tech Scholar, [2]Head of Department
Department of Electrical Engineering
Jind institute of Engineering & Technology Jind Haryana
[1]monujulani002@gmail.com, [2]pankaaaz@gmail.com

Abstract: The main element is a photovoltaic system that is designed to satisfy the daily load energy requirement. A three-phase active filter is used to improve the power quality, manage the power, and correct the unbalance. Backup energy storage systems including plug-in hybrid electric vehicles and the diesel generator are used to ensure an uninterruptible power supply in case of low solar irradiation. Microgrid systems became an important solution to reach remote areas and maximize the economic, technological, and environmental benefits. In this paper, a grid connected solar charger is designed for charging of electric vehicles. For getting the maximum power from the solar system, Perturb and Observe (P & O) MPPT technique has been implemented. The results are obtained in forms of grid outputs, solar outputs, battery charging and discharging and SOC of battery. The proposed model is implemented on MATLAB software.

Keywords: Load Dispatch, Genetic Algorithm, ALO, single-zone thermal power plant, Optimization, PSO.

1. INTRODUCTION

Electric vehicles are widely used because of their greater benefits such as easy maintenance, lower running cost, and environmental pleasant. The storage of electrical energy in rechargeable batteries is the main source to propel electric motors present in an electric automobile. The 1880s was the year of the invention but popularized in the 20th century as an advance of internal combustion engines. In 1987, electric cars found their commercial use in the USA and it does not require gear exchange when compared with conventional vehicles. Characteristics of an electric vehicle depend on the battery size and electric range of utilization [1]. There is no tailpipe emission when compared with IC engines which in turn reduces the greenhouse gas emission-related issues. Significant reduction of air pollution in city areas is the result of EV usage because they do not emit pollutants including soot, hydrocarbons, carbon monoxide, volatile organic compounds, ozone, lead, and oxides of nitrogen. The pollutant emission is based on the emission intensity of charging sources as well as there is an energy wastage during the charging state. High power to weight ratios is the output of electric motors which require a heavy current supply. Fixed ratio gearboxes and clutch absence are the reason for the reliability and simplicity of the EV's. Acceleration capability is based on the size of motors and has constant torque [2]. Especially at low speeds, acceleration performance will be more relative to that of the same motor power internal combustion engine. The power rate increment relies on motor-to-wheel configuration because wheels directly have the connection with motors for propulsion & breaking.

1.1. RENEWABLE ENERGY

Easter, Biczel and & Klos (2009) Polish energy law, which regulates renewable energy such as the use of renewable energy, solar energy, hydropower, wave energy and waves, energy from rivers, biomass energy and energy in the conversion process produced in the process of burial biogas and treatment of contaminants and treatment of decay or damage to plants and animals. According to Musgrove (1983), wind energy is an independent form of solar energy, because wind is due to the presence of the equatorial surface of the earth more sun than Polar Regions, which will cause large tumors in the atmosphere the total amount of solar energy per year is enormous.

1.2. WIND ENERGY

Wind is defined as a series of wind waves, in which there are numerous aerial movements on Earth. Due to the irregular heat of the sun on the ground, the pressure difference in the wind leads to the wind. Rotation due to the power of Coriolis. (Getachew, 2009). The use of wind energy is an ancient technology; its history can be traced back to the Middle East 1400-1800 years ago. The first application of wind energy includes the use of wind energy for agriculture, navigation and other irrigation.

1.3. SOLAR PV ELECTRICITY GENERATION

Solar power is the conversion of energy from the sun to electricity. Among the main expansions in converting solar power into useful energy, the forms include the direct conversion of solar energy to electricity using the photovoltaic effect (Garcia-Lopez et al., 2015). Another wide application of indirect solar energy conversion is the manufacture of heat mostly in form of Concentrated Solar Power (CSP).

1.4. ELECTRIC VEHICLE COORDINATION

If there is a large series of vehicles in operation, the provision of additional services from electric vehicles is a very viable option [40] As Kempton et al. [40] In 2001, due to power restrictions, only one electric vehicle was able to enter the power market or establish a business relationship with the power agency.

There are many reasons behind the installation of electric car chargers. First, in the current market situation, individual participation in small groups is prohibited. In addition, it allows for the simplest connection to the DSO in troubleshooting. The use of appropriate strategies can reduce the risk of traffic accidents.

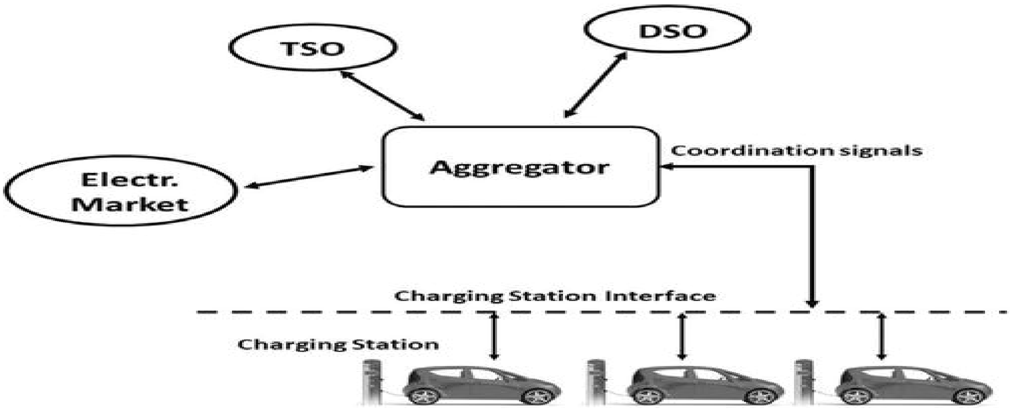

Figure 1. Simplified EV coordination framework: transmission system operator (TSO), distribution system operator (DSO), electric market, and charging stations for EVs.

With the increase in PV penetration of low-power power lines, EV load control can improve feeder performance and reduce investment requirements for infrastructure upgrades. In plates with such a high permeability, there is a constraint to keep in mind. The customer will evaluate the improvement in reliability, quality, and price. We expect a significant change in the quality of power in the near future, which aims to reduce the long-term changes in power growth that occur in the environment of decentralized RES production. In theory, we know that balancing car loads can promote a local balance between production and consumption, which can reduce power shortages and overheat.

2. PROPOSED EV MODEL

Optimization Will Be Based on Minimizing the Summation of Total Electricity Cost from Power Grid

Battery life, safety, and reliability are all important if the battery is charged and discharged properly. In this paper, the bidirectional power converters are used to figure out how to manage the power of a PHEV battery in a different way. Up to 10A can be used to charge a battery with this system. It can also send power back to the single-phase 230V, 50 Hz power at a rate of 10A. Two parts make up the system: a single-phase AC-DC converter and a DC-DC converter. A single-phase bidirectional AC-DC converter is used to change AC voltage to DC voltage. To charge, the DC-DC converter goes into buck mode. To discharge, the converter goes into boost mode. The charging and discharging of the battery show how the battery works.

Uncoordinated charging of electric vehicles can result in a massive electric load on the grid, resulting in increased power system peak load and distribution grid congestion. The production of renewable energy and the coordination of EV charging have been investigated in order to avert such a scenario. To be more precise, the study examined EV-based solutions for providing ancillary services in conjunction with wind integration and energy storage in conjunction with photovoltaic integration.

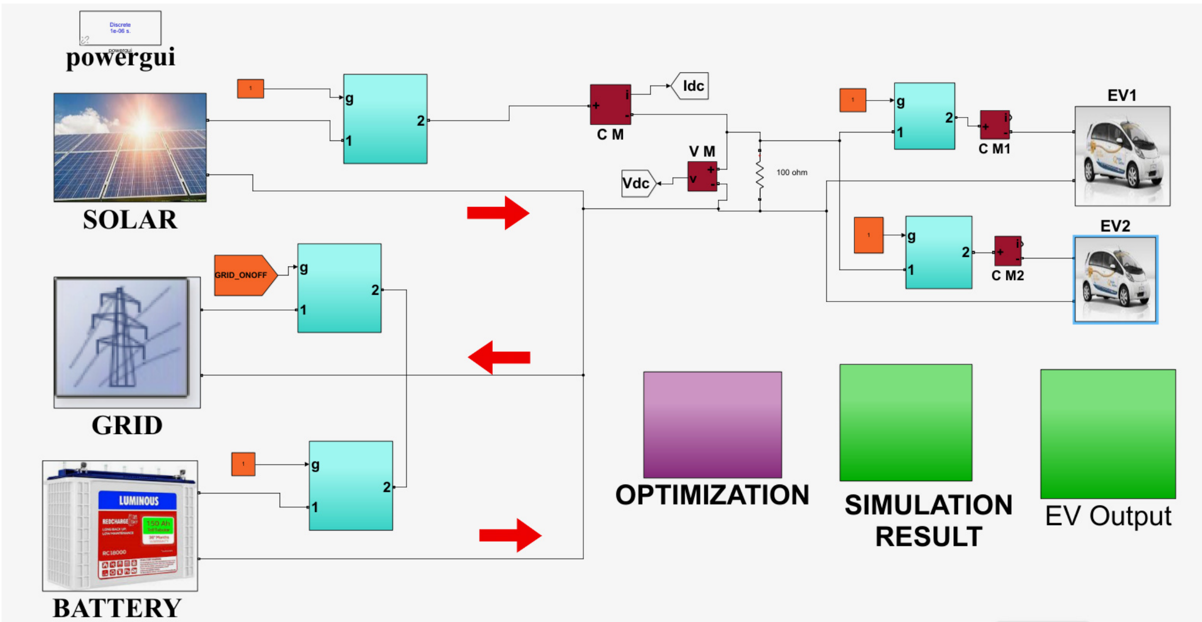

Figure 2. Proposed MATLAB Simulink model

Modules

- Solar power
- MPPT Algorithm
- Boost converter
- Grid
- Bidirectional converter
- Battery
- PWM Switching

Table 1. Battery Parameters

Parameter	**Value**
Nominal voltage (V)	150
Rated capacity (Ah)	150
Initial state-of-charge (%)	90
Battery response time (s)	30
Discharge	
Maximum capacity (Ah)	150
Cut-off Voltage (V)	112.5
Fully charged voltage (V)	174.5981
Nominal discharge current (A)	65.2174
Internal resistance (Ohms)	0.01
Capacity (Ah) at nominal voltage	135.6522
Exponential zone [Voltage (V), Capacity (Ah)]	[62.0579 7.3695]
Discharge current [i1, i2, i3,...] (A)	[6.5 13 32.5]

3. RESULT & DISCUSSION

This section of the article contains the obtained results;

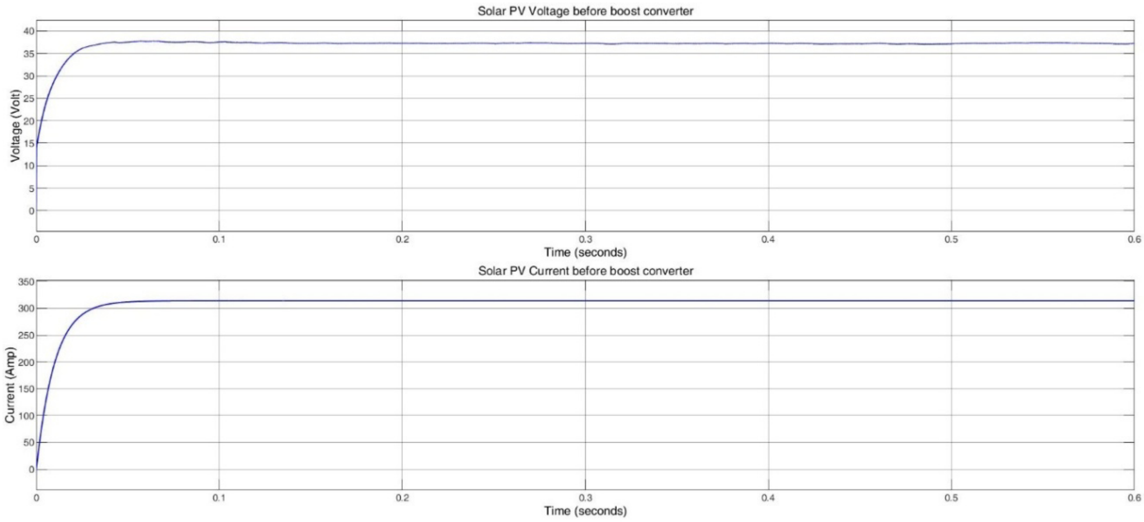

Fig. 3. Solar PV voltage and current waveform before the boost converter

Fig 3 solar voltage and current waveform before the boost converter, the current generated 315 A, Where Voltage generated 37.2 V from the solar.

The voltage waveform of a solar panel is relatively stable in steady sunlight conditions. It shows a direct current (DC) voltage level with slight fluctuations due to changes in sunlight intensity. During the daytime, when the solar panel receives sunlight, the voltage output remains positive and can vary based on factors like the number of cells in the panel, the quality of the sunlight, and the temperature. The current waveform of a solar panel is also direct current (DC), and it correlates with the intensity of sunlight. As the sunlight's intensity changes throughout the day, the current output of the solar panel also changes. During periods of high sunlight intensity (sunny conditions), the current output is higher, and during periods of lower intensity (cloudy or shaded conditions), the current output decreases.

International Journal of Engineering Research Excellence and Applied Science (IJEREAS)

Volume-II (Issue 2) - June 2024 ISSN: 3048-5355

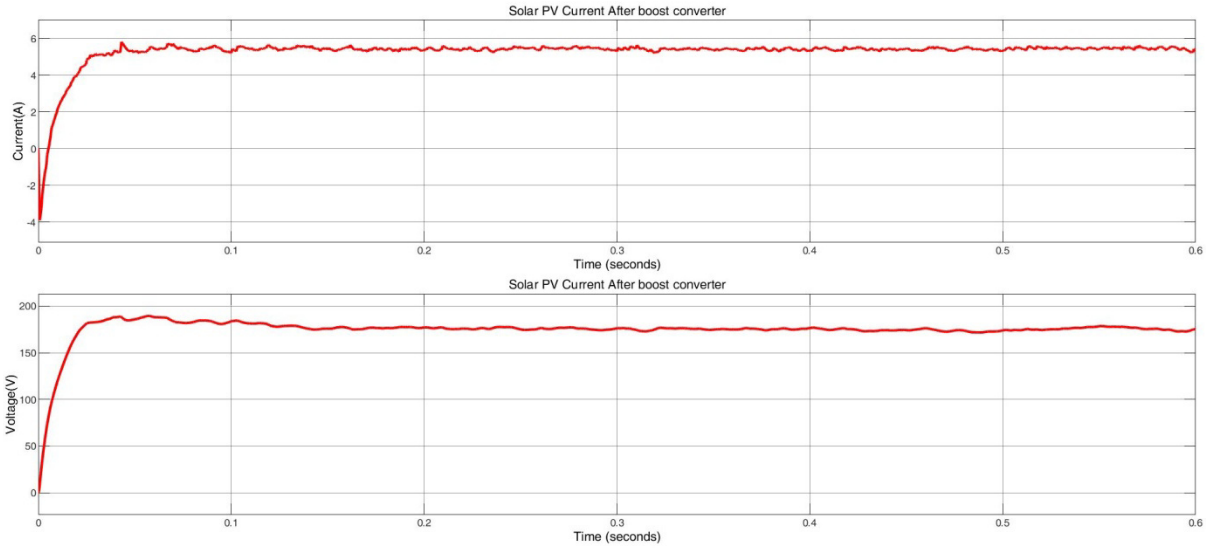

Fig 4. Solar PV voltage and current waveform after Boost Converter

Fig 4 showing the solar voltage and current waveform after the converter, the current generated 5.3 A, Where Voltage boosted form 37.2 V to 170 V from the solar.

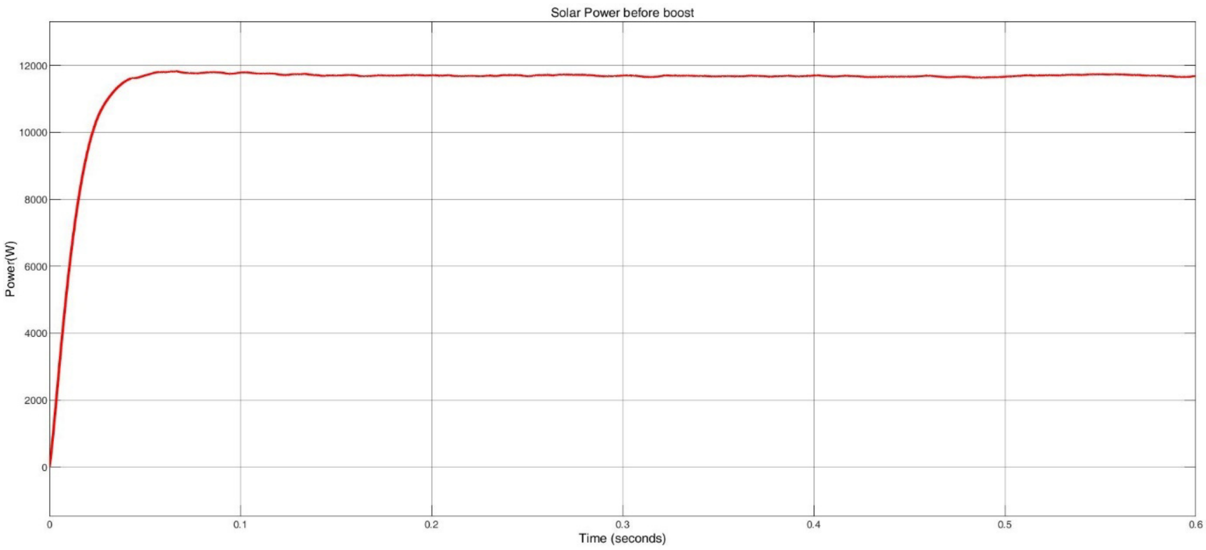

Fig 5. Solar PV Power before Boost Converter

International Journal of Engineering Research Excellence and Applied Science (IJEREAS)
Volume-II (Issue 2) - June 2024 ISSN: 3048-5355

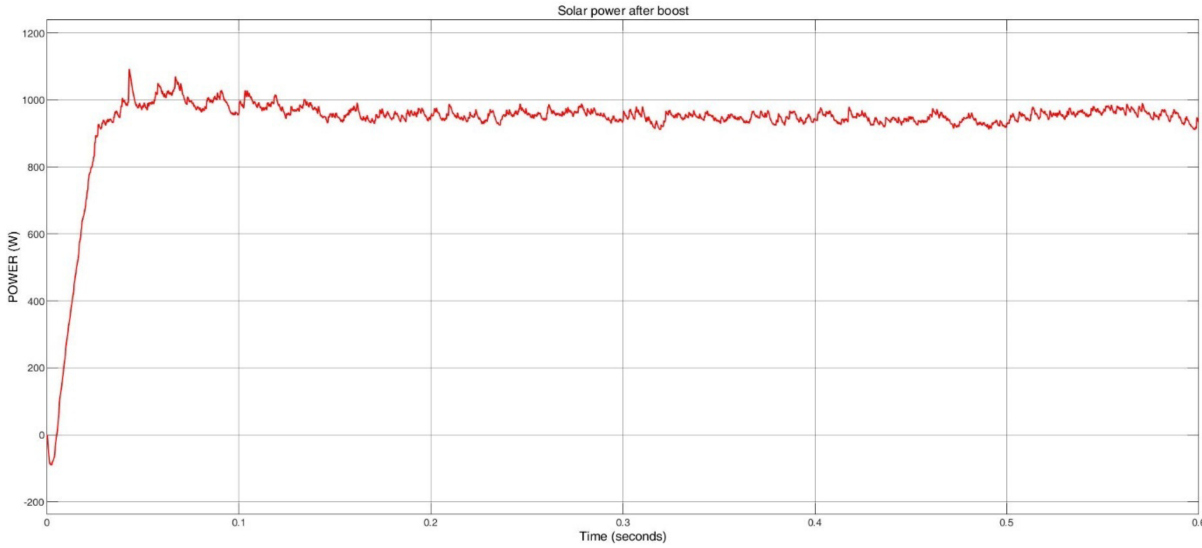

Fig 6 Solar PV Power after Boost Converter

The voltage waveform after conversion through an inverter is a sinusoidal AC waveform. The magnitude of the voltage varies according to the grid's voltage levels (e.g., 120V or 240V in residential systems). The frequency of the waveform is typically 50 or 60 Hz, depending on the region. The current waveform after conversion is also sinusoidal and follows the same frequency as the voltage waveform. However, the magnitude of the current waveform depends on the load being supplied by the solar-generated electricity. In a well-designed system, the current waveform matches the voltage waveform in phase and frequency, ensuring efficient and stable power transfer.

Battery behavior at Initial SOC of 10%

In this scenario, the battery's initial SOC is 10%. The battery is being charged, meaning energy is being added to the battery to increase its SOC. The SOC increases from 10% to a higher level as the battery receives more energy. Battery volage and current will be at 161.5 V and -667 A respectively. Negative current shows that battery is charging.

International Journal of Engineering Research Excellence and Applied Science (IJEREAS)

Volume-II (Issue 2) - June 2024 ISSN: 3048-5355

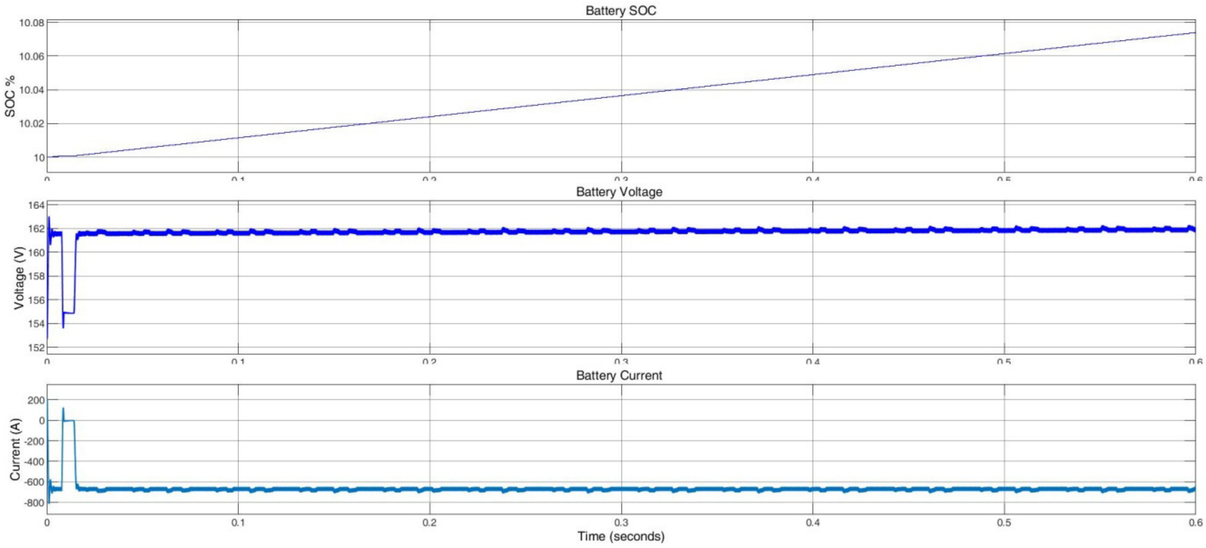

Fig.7 Battery SOC, Voltage and Current at initial SOC of 10%

Battery behavior at Initial SOC of 40%

The battery's initial SOC is 40% showing in fig 5.6. The battery is being charged, meaning energy is being added to the battery to increase its SOC. The SOC increases from 40% to a higher level as the battery receives more energy. Now battery voltage will be increase from 161.5 V to 169 V, and current remains same.

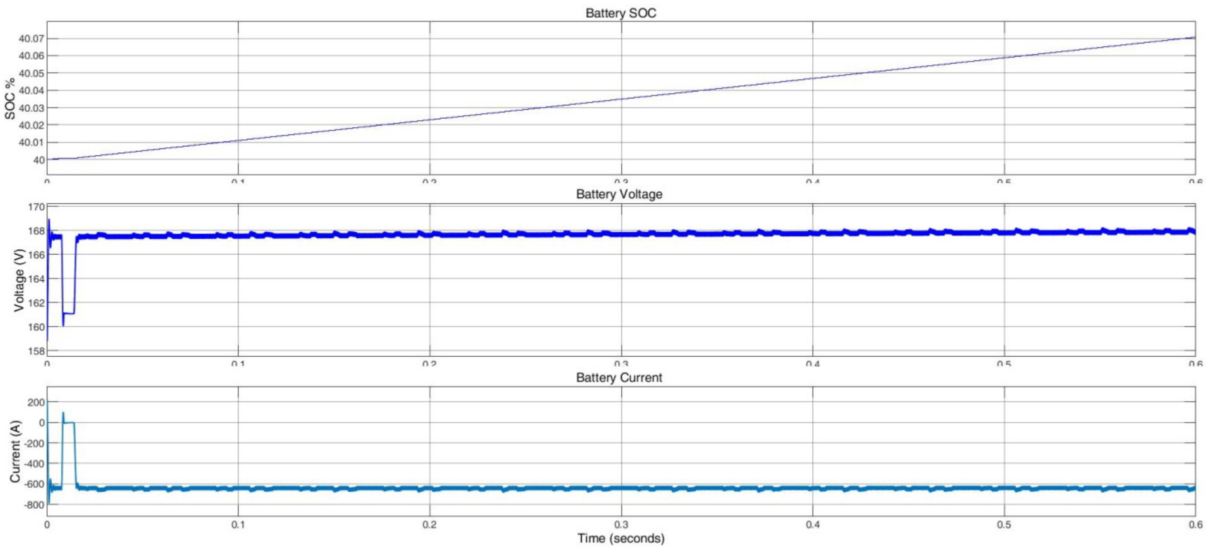

Fig.8 Battery SOC, Voltage and Current at initial SOC of 40%

Battery behavior at initial SOC of 75%

International Journal of Engineering Research Excellence and Applied Science (IJEREAS)

Volume-II (Issue 2) - June 2024 ISSN: 3048-5355

Battery will be in Initial charging mode as shown in fig. 5.7. Now battery voltage will be increase from 168.5 V to 169 V, and current decrease to -630 V. Battery will be charge slowly compare to SOC of 40%.

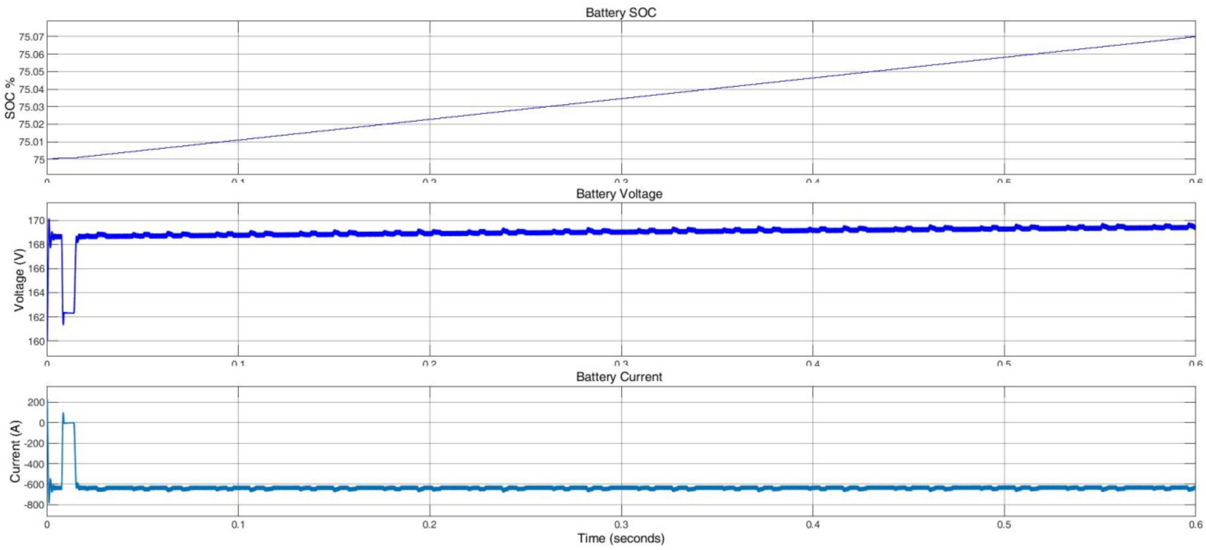

Fig.9.Battery SOC, Voltage and Current at initial SOC of 75%

Comparison of Battery behavior at initial SOC of 90% and 91%

From fig. 5.8 and fig. 5.9, at 90% SOC battery is charging but at 91% SOC battery start to discharging by giving power to load. Current will become positive to negative for SOC 90% and 91%.

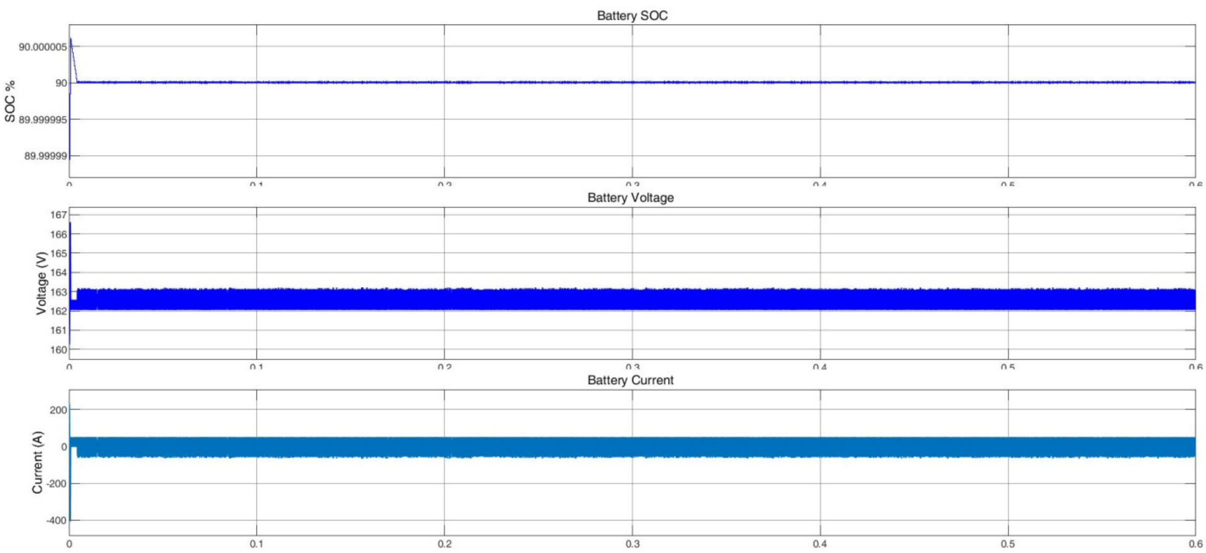

Fig.10. Battery SOC, Voltage and Current at initial SOC of 90%

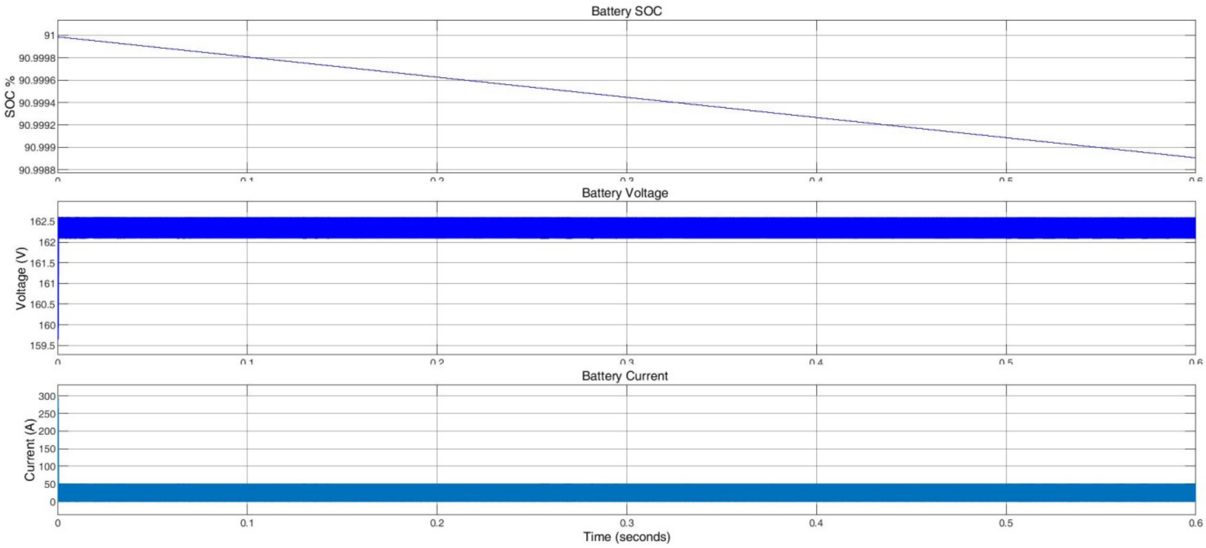

Fig. 11.Battery SOC, Voltage and Current at initial SOC of 91%

SOC Discharging at 100%: In this scenario, the battery's initial SOC is 100%. The battery is being discharged, providing energy until its SOC decreases to a specified level. Depending on the battery chemistry and management system, some batteries might not discharge all the way to 0% SOC to protect their longevity. showing in fig 11.

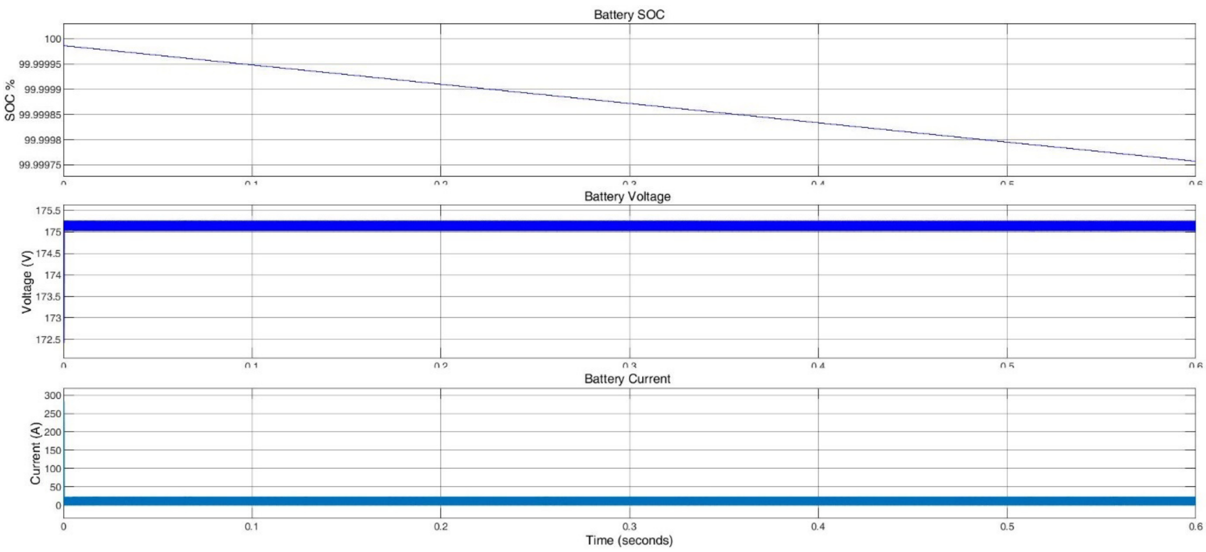

Fig. 12. Battery SOC, Voltage and Current at initial SOC of 100%

International Journal of Engineering Research Excellence and Applied Science (IJEREAS)
Volume-II (Issue 2) - June 2024 ISSN: 3048-5355

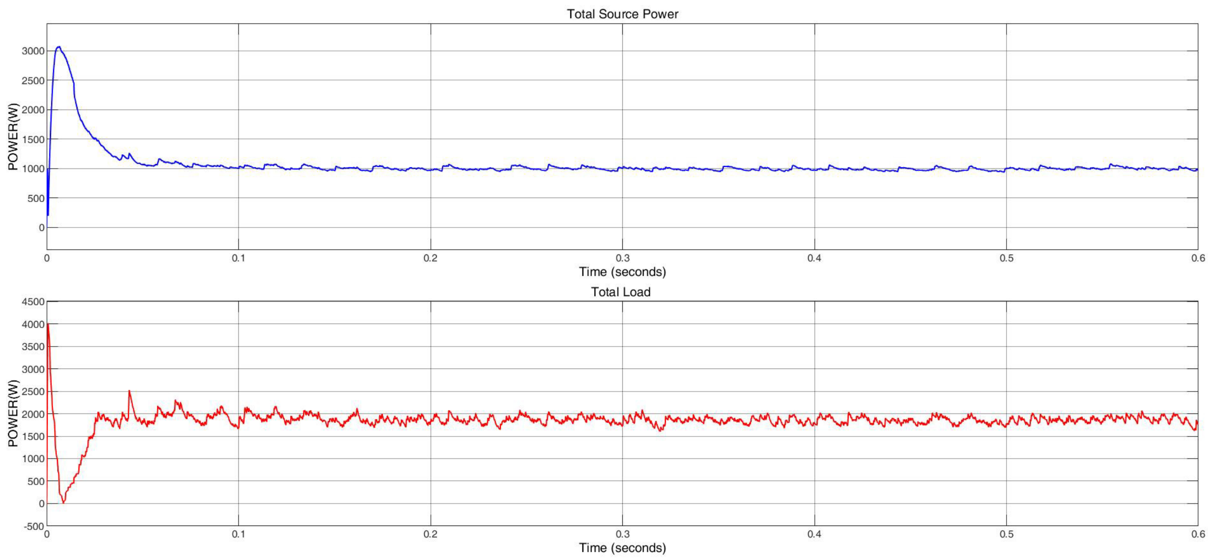

Fig. 13. Total source power and load power

Fig. 13 showing the total source power and total load power of the system, the total source power and the total load power refer to the total power being generated (source power) and the total power being consumed by devices or systems (load power).

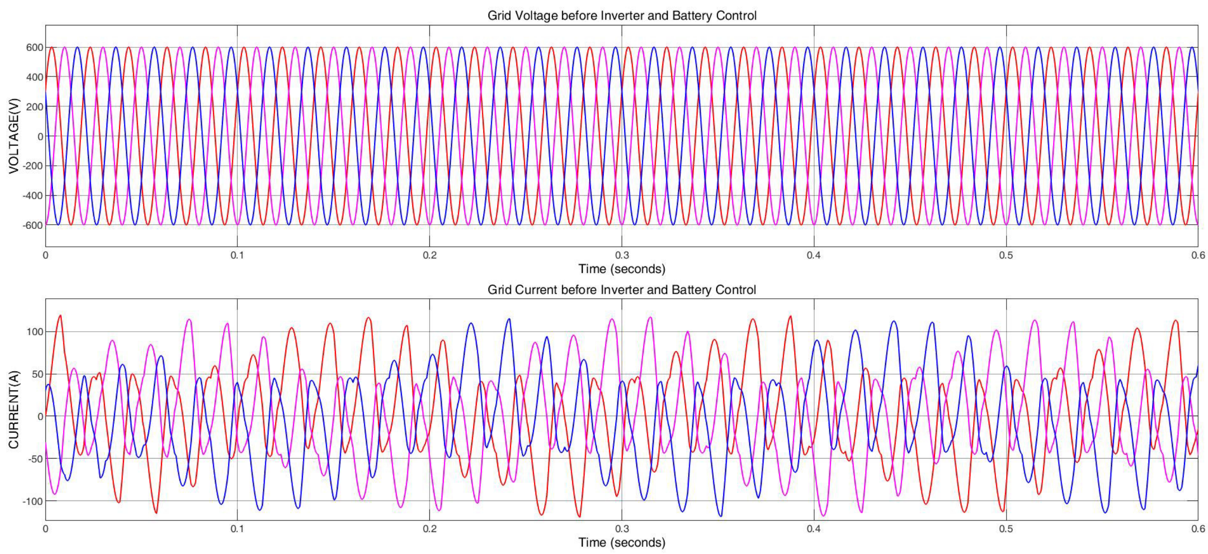

Fig. 14 Grid Voltage and current before Inverter and Battery Control

International Journal of Engineering Research Excellence and Applied Science (IJEREAS)
Volume-II (Issue 2) - June 2024 ISSN: 3048-5355

Fig 14 showing the grid voltage and current waveform before Inverter and Battery Control, the current generated 120 A, Where Voltage generated 600V, The grid voltage and current waveforms need to be synchronized with the overall grid's waveform to ensure proper power distribution and compatibility with other power sources and loads.

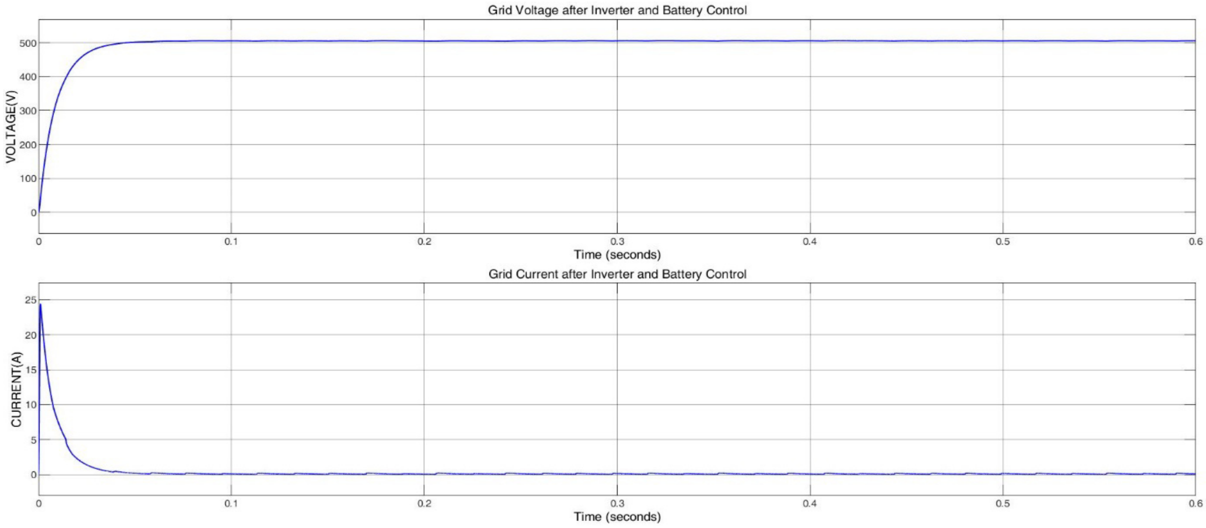

Fig. 15. Grid Voltage and current after Inverter and Battery Control

Fig 15 showing the grid voltage and current waveform before converter, the current generated 1 A, Where Voltage generated 500V. The grid voltage and current waveforms need to be synchronized with the overall grid's waveform to ensure proper power distribution and compatibility with other power sources and loads.

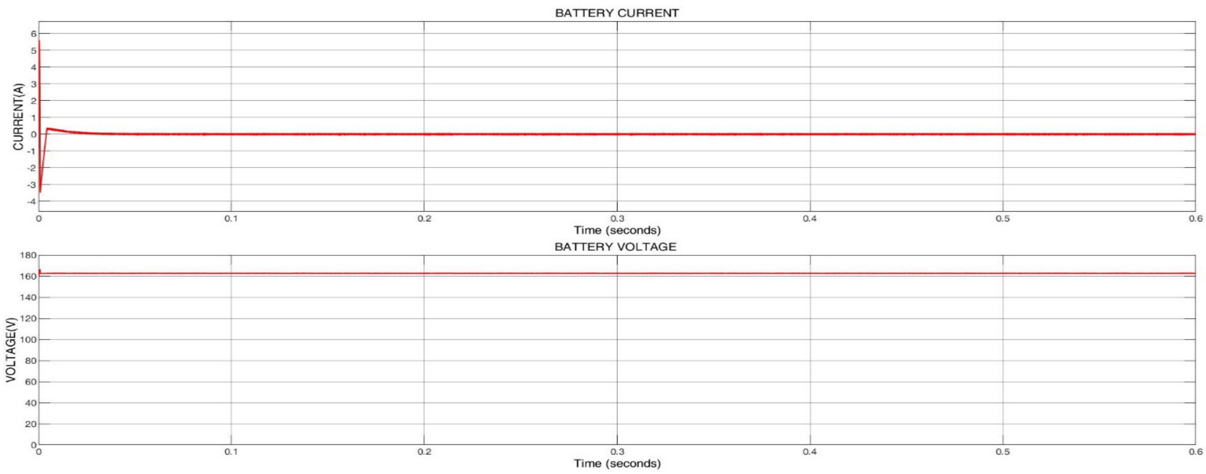

Fig. 16 Battery voltage and current of the system

International Journal of Engineering Research Excellence and Applied Science (IJEREAS)

Volume-II (Issue 2) - June 2024 ISSN: 3048-5355

The battery voltage waveform can be relatively stable during steady-state conditions. As the battery charges, the voltage tends to rise, reaching its peak voltage when the battery is fully charged. During discharging, the battery current waveform starts high and decreases as the battery's SOC reduces.

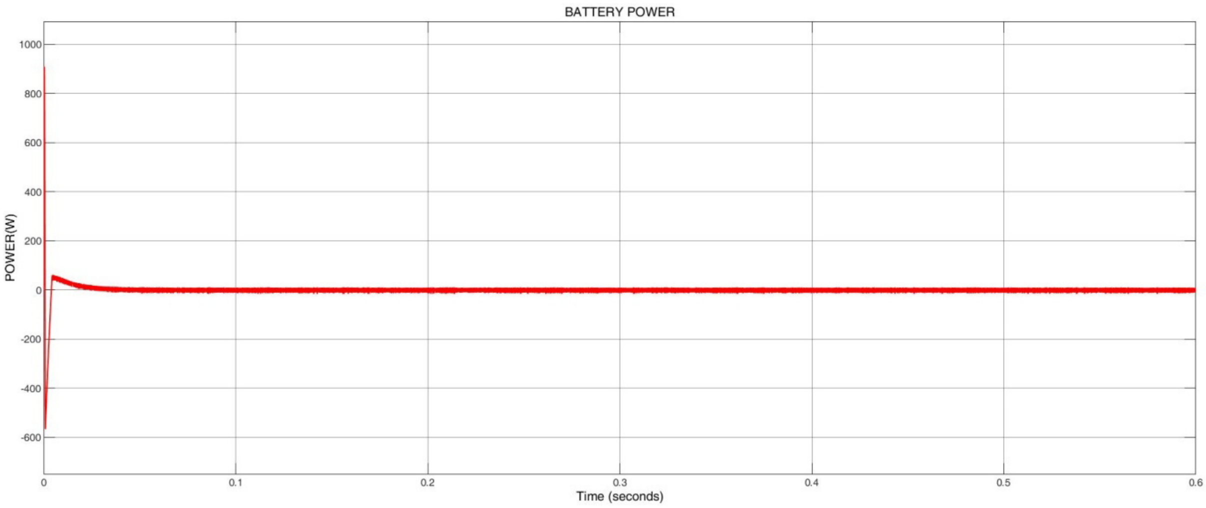

Fig. 17. Battery power generate by the system at SOC 90%

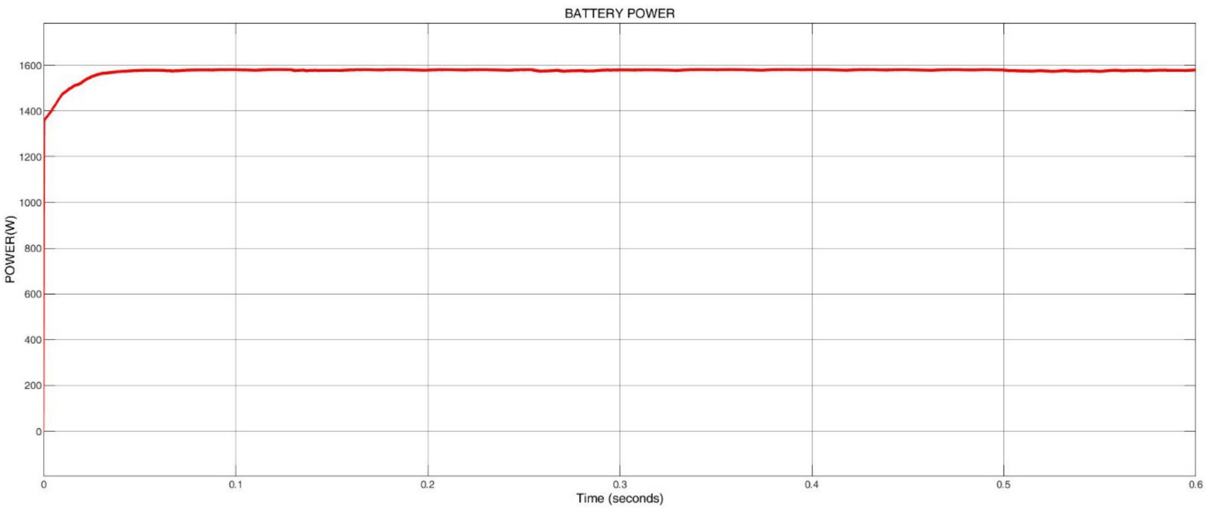

Fig. 18. Battery power generate by the system at SOC 91%

The x-axis represents time, showing the progression of the discharging process. The y-axis represents power in watts (W), indicating the rate at which energy is being delivered by the battery to the load.

At 90% SOC battery power is very small and at 91% SOC it delivering constant power to load 1570 Watt, fig. 5.15 and 5.16.

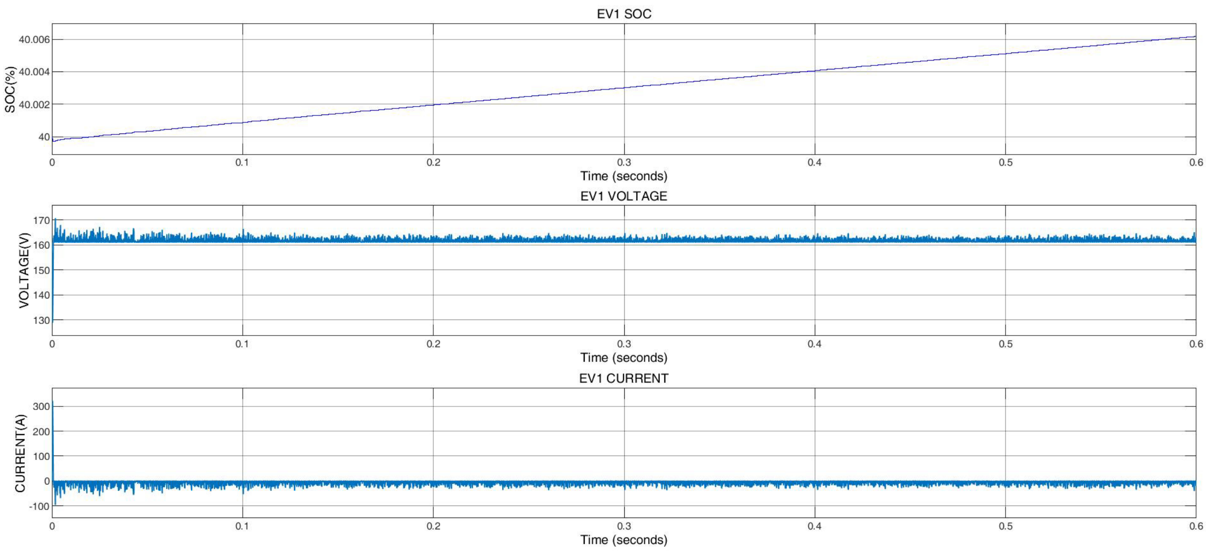

Fig. 19. Battery SOC, Battery voltage and battery current for EV1 Station

The x-axis represents time, showing the progression of the operational phases. The y-axis on the left side represents battery SOC as a percentage (%), indicating the amount of energy remaining in the battery. The y-axis on the right side represents battery voltage in volts (V), indicating the electrical potential difference of the battery. The battery current is represented by the data points on the graph.

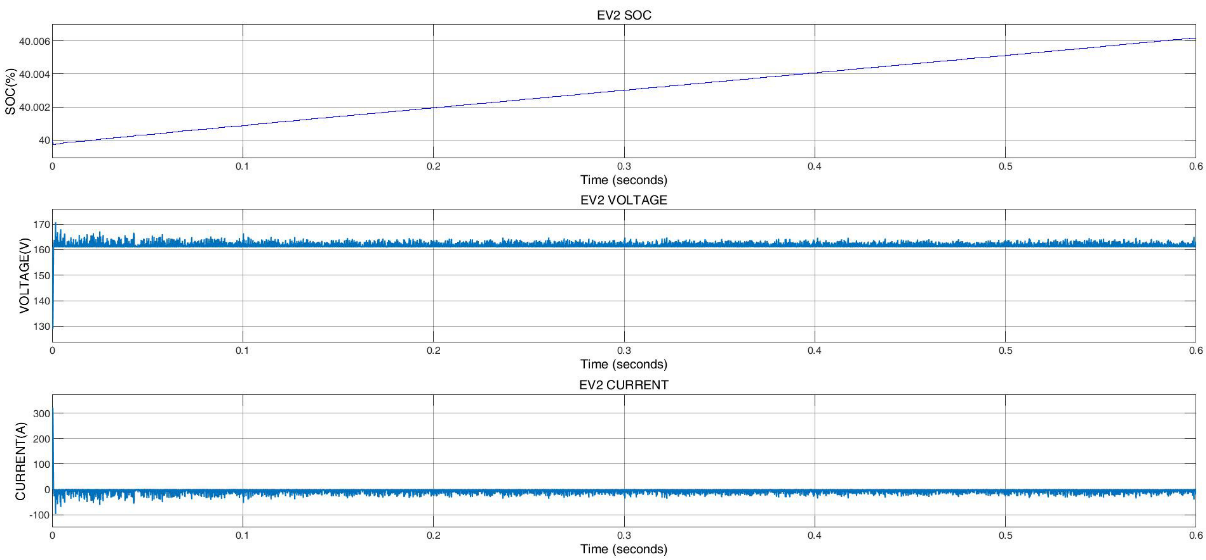

Fig. 20 Battery SOC, Battery voltage and battery current for EV2 Station

International Journal of Engineering Research Excellence and Applied Science (IJEREAS)

Volume-II (Issue 2) - June 2024 ISSN: 3048-5355

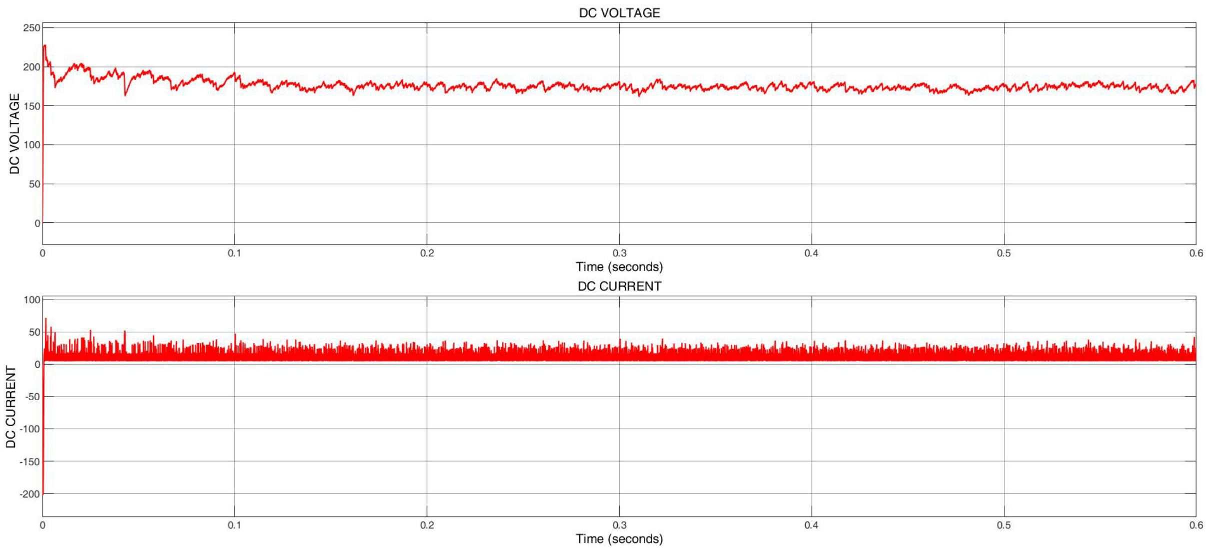

Fig. 21. DC voltage and current

Fig 21 showing generated DC voltage and current from the Simulink model. The x-axis represents time, showing the progression of the operational phases. The y-axis on the left side represents DC voltage in volts (V), indicating the electrical potential difference. The y-axis on the right side represents DC current in amperes (A), indicating the flow of electric charge.

4. FUTURE SCOPE

Research and development is a continual and relentless process. For any research work already carried out, there is always room for improvement, which opens up many avenues for further research. As a result of the research in this paper, the following aspects are determined to further the research work.

- Current work can be extended through various energy storage, such as battery storage systems (BESS) and power-saving systems (SMESS) for AGCs.
- It can be seen at the nominal value that the proposed observer is very strong in many standards and functional limitations. And finally, by considering the physical constraints such as delaying time and repositioning the gas turbine, the proposed method will be expanded to a more robust power model.
- Various methods can be used to realize the wireless connection to the car to eliminate the difficulty of unlocking.
- SC-Bank location can be used for heavy-duty vehicles and stand-up and vehicle testing.
- Other customizable ways to choose the rotation of the car.
- The fixed lanes of the vehicle can be projected to reach the maximum rate of renewal rate and rate of application.

The Fixed Route, with and without a driver can be tested and the regeneration, as well as utilization of the energy, can be estimated. In the battery management of the hybrid vehicle, the future work can be extended to integrating concepts of the battery management system and power management that can be controlled with the state of charge, controlling the power flow. The state of charge can be controlled with different types of controllers like PI, PID, and fuzzy controllers and can also be extended to the artificial neural networks. The vehicle can also be analyzed with different types of converters with different switching designs where a higher gain can be obtained. A vehicle can also be analyzed with different multilevel inverters and so the total harmonic distortion of the output of the inverter can be decreased. Also, the motor drive for the vehicle can be realized with different controllers to obtain control over the speed and reduction of torque ripples.

REFERENCES

1. Fadoul Souleyman Tidjani, Abdelhamid Hamadi, Ambrish Chandra*, Fellow IEEE, Benhalima Saghir, Energy Management of Micro Grid-based Electrical Vehicle to the Building (V2B) 978-1-7281-5152-6/19/$31.00 ©2019 IEEE.
2. Q. Xu, J. Xiao, P. Wang, X. Pan, and C. Wen, “A decentralized control strategy for autonomous transient power-sharing and state-of-charge recovery in hybrid energy storage systems,” IEEE Trans. Sustain. Energy, vol. 8, no. 4, pp. 1443–1452, Oct 2017.
3. K. Thirugnanam, S. K. Kerk, C. Yuen, N. Liu, and M. Zhang, “Energy management for a renewable microgrid in reducing diesel generators usage with multiple types of battery,” IEEE Trans. Ind. Electron., vol. 65, no. 8, pp. 6772–6786, Aug 2018.
4. Y. Liu, C. Yuen, N. U. Hassan, S. Huang, R. Yu, and S. Xie, “Electricity cost minimization for a microgrid with distributed energy resource under different information availability,” IEEE Trans. Ind. Electron., vol. 62, no. 4, pp. 2571–2583, April 2015
5. X. Xu, Q. Liu, C. Zhang, and Z. Zeng, “Prescribed performance controller design for dc converter system with constant power loads in dc microgrid,” IEEE Trans. Sys., Man, and Cyber.: Sys., pp. 1–10,2018.
6. D. K. Dheer, S. Doolla, and A. K. Rathore, “Small-signal modeling and stability analysis of a droop based hybrid ac/dc microgrid,” in IECON2016 - 42nd Annual Conf. of the IEEE Ind. Electron. Society, Oct 2016, pp. 3775–3780.
7. SrikanthKotra and Mahesh K. Mishra, “A supervisory power management system for a hybrid microgrid with hess,” IEEE Trans. Ind.Electron., vol. 64, no. 5, pp. 3640–3649, May 2017.
8. R. W. Erickson and D. Maksimovic, Fundamentals of power electronics.Springer Science & Business Media, 2007.
9. R. Kötz and M. Carlen, “Principles and applications of electrochemical capacitors,” Electro Chim. Acta, vol. 45, no. 15–16, pp. 2483–2498, 2000.
10. J. W. Dixon, M. Ortúzar, and E. Wiechmann, “Regenerative braking for an electric vehicle using ultracapacitors and a buck-boost converter,” in Proc. EVS18, Berlin, Germany, Oct. 2001, pp. 148.

11. Hong G, Yi-min G, and Ehsani M. A neural network-based SRM drive control strategy for regenerative braking in EV and HEV. In: Electric machines and drives conference, IEMDC 2001, Cambridge, MA, pp.571–575, 17–20 June 2001.
12. J. W. Dixon and M. Ortúzar, “Ultra capacitors+ DC-DC converters in a regenerative braking system,” IEEE Aerosp. Electron. Syst. Mag., vol. 17, no. 8, pp. 16–21, Aug. 2002.
13. Gao, L., Dougal, R.A., and Liu, S., Active Power Sharing in Hybrid Battery/Capacitor Power Sources, in Applied Power Electronics Conference and Exposition, APEC'03, Eighteenth Annual IEEE, 1, pp. 497-503, 2003.
14. G. L. Plett, “Extended Kalman filtering for battery management systems of LiPB-based HEV battery packs—part 1. Background,” Journal of Power Sources, vol. 134, no. 2, pp. 252–261, 2004.
15. S. Ban, J. Zhang, L. Zhang, K. Tsay, D. Song, and X. Zou, “Charging and discharging electrochemical supercapacitors in the presence of both parallel leakage process and electrochemical decomposition of solvent,” Electro Chimica Acta, vol. 90, pp. 542–549, 2013.
16. Wu, X., Du, J., and Hu, C. “Energy Efficiency and Fuel economy Analysis of a Series Hybrid Electric Bus in Different Chinese City Driving Cycles” International Journal of Smart Home, Vol. 7, No. 5, pp 353-368, 2013.
17. Y. M. Nie and M. Ghamami, "A corridor-centric approach to planning electric vehicle charging infrastructure," Transportation Research Part B: Methodological, vol. 57, pp. 172–190, November 2013.
18. . L. Jian, et al., "A scenario of vehicle-to-grid implementation and its double-layer optimal charging strategy for minimizing load variance within regional smart grids," Energy Conversion and Management vol. 78, pp. 508–517, February 2014.
19. L. Zhang, W. Zhenpo, F. Sun, and D. Dorrell, “Ultracapacitor modeling and parameter identification using the extended Kalman filter,” ITEC Asia Pacific vol. 7, pp. 3204–3217, 2014.
20. Y. Wei, J. Zhu, and G. Wang, “High-specific capacitance supercapacitor base on vanadium oxide nanoribbon,” IEEE Trans. Appl. Super cond., vol. 24, no. 5, 2014.
21. Burke, A.F., “Present and future supercapacitors: Technology and applications” presentation at the Supercapacitor USA 2014, Santa Clara, California, November 2014.
22. L. Zhang, Z. Wang, F. Sun, and D. G. Dorrell, “Online parameter identification Of ultracapacitor models using the extended Kalman filter,” Energies, vol. 7, no. 5, pp. 3204–3217, 2014.
23. Dubal, D.P., Ayyad, O., Ruiz, V., and Gomez Romero, P., Hybrid Energy Storage: The Merging of Battery and Supercapacitor Chemistries, Chemical Society Reviews, vol.44, no.7, pp. 1777-1790, 2015.